

Testing common classical LTE and NLTE model atmosphere and line-formation codes for quantitative spectroscopy of early-type stars

Norbert Przybilla¹, Maria-Fernanda Nieva^{1,2} and Keith Butler³

¹ Dr. Karl Remeis-Sternwarte & ECAP, Sternwartstr. 7, D-96049 Bamberg, Germany

² Max-Planck-Institut für Astrophysik, Karl-Schwarzschild-Str. 1, D-85741 Garching, Germany

³ Universitätssternwarte, Scheinerstr. 1, D-86179 München, Germany

E-mail: norbert.przybilla@sternwarte.uni-erlangen.de

Abstract. It is generally accepted that the atmospheres of cool/lukewarm stars of spectral types A and later are described well by LTE model atmospheres, while the O-type stars require a detailed treatment of NLTE effects. Here model atmosphere structures, spectral energy distributions and synthetic spectra computed with ATLAS9/SYNTHÉ and TLUSTY/SYNSPEC, and results from a hybrid method combining LTE atmospheres and NLTE line-formation with DETAIL/SURFACE are compared. Their ability to reproduce observations for effective temperatures between 15 000 and 35 000 K are verified. Strengths and weaknesses of the different approaches are identified. Recommendations are made as to how to improve the models in order to derive unbiased stellar parameters and chemical abundances in future applications, with special emphasis on Gaia science.

1. Introduction

Quantitative stellar spectroscopy employs model atmospheres that are based on many approximations and simplifications. One of the fundamental decisions to be made for the model construction concerns the description of the thermodynamic state of the atmospheric plasma. Either local thermodynamic equilibrium (LTE) may be assumed, or deviations from it may be allowed for (NLTE), i.e. taking the mutual interaction of radiation and matter into account.

It is generally accepted that the atmospheres of cool/lukewarm stars of spectral types A and later are described well by LTE model atmospheres, while O stars require a detailed treatment of NLTE effects due to the high energy density of their radiation field. Both approaches are being followed in the literature for analyses of B-type stars at present, with variable success.

The present work tests the predictive power of common LTE and NLTE model atmosphere and line-formation codes in this transition region, concentrating on main-sequence stars of effective temperatures between 15 000 and 35 000 K (corresponding to spectral types of about B4 to O9). Three approaches are investigated: pure LTE as implemented in the ATLAS9/SYNTHÉ suite of codes [1, 2], pure NLTE with TLUSTY/SYNSPEC [3], and a hybrid approach based on LTE atmospheres (ATLAS9) and subsequent NLTE line-formation computations with DETAIL/SURFACE [4, 5]. We deviate from the usual ‘model vs. model’ comparison – which may be misleading as *a priori* it is not clear as to which model is more realistic – by testing observational constraints wherever possible.

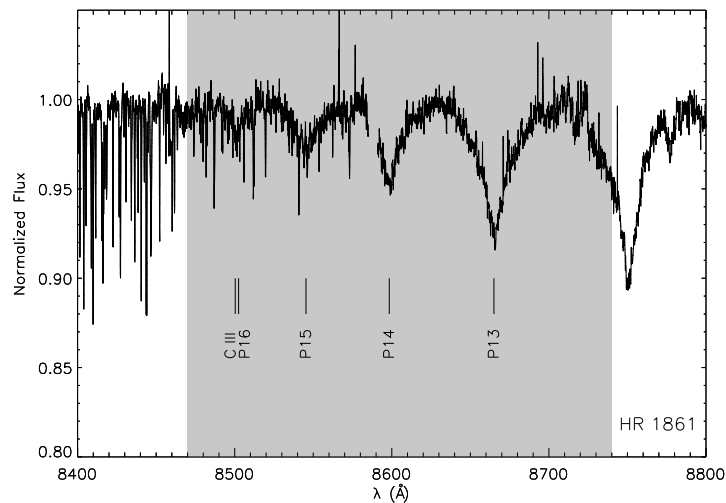


Figure 1. Near-IR spectrum of HR 1861 (B1 IV), observed with FOCES on the Calar Alto 2.2m telescope. The most important lines in the Gaia RVS spectral range (grey region) are identified.

2. The Gaia perspective for investigations of OB-type stars

The legacy of the Gaia mission in terms of OB-type stars will mainly lie in the determination of highly precise parallaxes, proper motions and broad-band space photometry. In contrast to the cooler stars, little information besides radial and projected rotational velocities will be derivable from the spectra obtained with the on-board radial-velocity spectrometer (RVS). The reason for this is the scarcity of spectral lines in the wavelength range of the RVS, which essentially comprises the Paschen series members P_{13} to P_{16} in this kind of star, see Fig. 1. The determination of accurate and precise stellar parameters and elemental abundances will therefore have to rely on ground-based observations, e.g. within the Gaia-ESO survey [6].

3. Models: assumptions & implementations

Quantitative spectroscopy of early-type main-sequence stars and giants in the effective temperature range of interest, $15\,000 \leq T_{\text{eff}} \leq 35\,000$ K, can rely on *classical model atmospheres*¹. Basic assumptions for the model construction are chemical homogeneity, stationarity, plane-parallel geometry and hydrostatic and radiative equilibrium, while the thermodynamic state of the atmospheric plasma can be determined in LTE or NLTE. The former case is conceptually less realistic but attractive since typical computing times per model are a few seconds on modern PCs, while NLTE models may require many CPU hours. A third approach, so-called hybrid NLTE modelling, can combine the strengths of both types of models, performing sophisticated NLTE line-formation computations on LTE atmospheres, at a fraction of the computing cost of full NLTE models. This is particularly attractive in those cases where the atmospheric structure is close to LTE as for the parameter space investigated here which we will show in the following.

For our test we have chosen results from the most common among the many available model atmosphere codes: on the one hand line-blanketed LTE atmospheres and synthetic spectra computed with the ATLAS9/SYNTH3 suite of codes [1, 2] and on the other line-blanketed NLTE models calculated with the TLUSTY/SYNSPEC package [3]. Model structures, fluxes and detailed synthetic spectra were adopted from published grids, Castelli’s ODFNEW models [8], the Padova spectral library [9], and the OSTAR2002 and BSTAR2006 grids [10, 11].

¹ More luminous stars, either mid/early O-type stars or OB-supergiants close to the Eddington limit, require consideration of their stellar winds, i.e. hydrodynamic model atmospheres (and spherical geometry), see e.g. [7].

Table 1. Model atoms used with our DETAIL/SURFACE computations.

Ion	Ref.	Ion	Ref.	Ion	Ref.	Ion	Ref.
H I	[13]	C II/III	[15, 16]	O I/II	[18, 19]	Si III/IV	[21]
He I/II	[14]	N II	[17]	Mg II	[20]	Fe II/III	[22, 23]

Our own computations rely on ATLAS9 atmospheres and NLTE line-formation computations with updated and extended versions of DETAIL/SURFACE [4, 5]. The former solves the coupled statistical equilibrium and radiative transfer equations, employing the accelerated lambda iteration scheme of [12], while the latter computes the synthetic spectra, using refined line-broadening theories. Model atoms according to Table 1 were employed. More details on our hybrid NLTE approach (labeled ‘ADS’ henceforth) can be found e.g. in [24].

4. Model tests

In order to facilitate the use of existing grids for the model comparisons, a two-step strategy has to be followed. In the first step, we compare our *tailored* ADS modelling with observation for strategic points in the investigated parameter space to test its ability to reproduce observation. Then, in the second step, ADS models for *generic* parameters are compared to the TLUSTY/SYNSPEC and ATLAS9/SYNTHÉ models at a grid point closest to the real star’s parameters, thus facilitating a meaningful assessment of the predictive power of all these modelling implementations. While the synthetic spectra were convolved with the same rotational and macroturbulent broadening profiles as for the comparison with observation, the Gaussian (‘instrumental’) profile had to be adjusted to account for the lower resolution of the Padova grid. Due to space restrictions we will discuss the case of the well-studied standard star γ Peg (B2 IV) in detail in the following, and comment on more general aspects of the comparisons briefly².

For γ Peg (HD 886) we derived $T_{\text{eff}} = 22\,000$ K, a surface gravity of $\log g = 3.95$ (cgs units), microturbulence $\xi = 2$ km/s, solar helium abundance and metal abundances typical for the normal early B-type star population in the solar neighbourhood [26, 28]. The nearest parameter combination covered by the published grids coincides with these, except that $\log g = 4.00$ and solar abundances according to [29]. We have adopted the generic grid parameters nevertheless for the ADS model in the second step of the comparison in order to avoid any systematic bias.

Model atmosphere structures and spectral energy distributions. We begin testing the models with a comparison of atmospheric structures in Fig. 2. The temperature structures of the LTE and NLTE models agree very well, except for the outermost layers. Differences amount to up to 1–2% for all depths relevant for the formation of the spectral lines and continua from the far-UV through the optical to the near-IR. Interestingly, the differences are smaller for the low-metallicity comparison at 1/10th of the solar value, despite the fact that NLTE effects should be more pronounced because of increased photon mean-free paths and a harder radiation field. A possible explanation of this unexpected finding could be the differences in the metal line opacities (which matter more at higher metallicity). Many more elements are considered in

² Our observational sample comprises a total of 29 apparently slowly-rotating B3 to B0 dwarf and giant stars, for which spectra of high signal-to-noise ratio ($S/N \sim 250\text{--}800$), high resolution ($R = \Delta\lambda/\lambda \simeq 40\text{--}48\,000$) and wide wavelength coverage were obtained using state-of-the-art Echelle spectrographs on 2m-class telescopes, see [25] for a brief overview. For this sample we have shown that combining a sophisticated analysis technique with our ADS modelling allows practically the entire observed spectra in the optical for all these objects [26, 27, 28] to be reproduced to similar or even better quality as shown for γ Peg in the following.

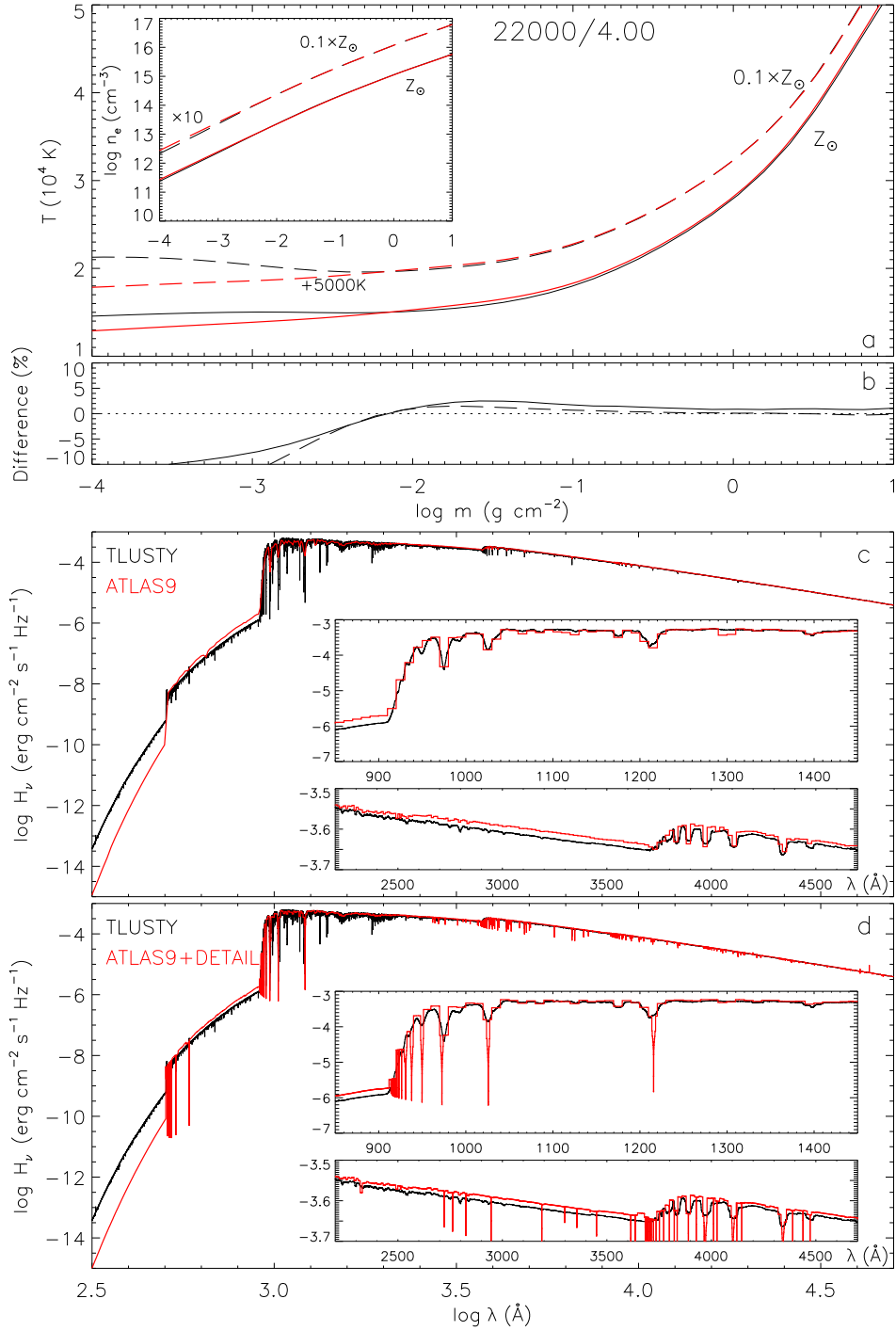


Figure 2. Comparison of model atmosphere structures and resulting spectral energy distributions. Panel (a) presents a comparison of ATLAS9 (red) and TLUSTY (black) temperature structures as a function of mass scale, for models at $T_{\text{eff}} = 22\,000$ K, $\log g = 4.00$, $\xi = 2$ km/s at solar (full lines) and 1/10th solar metallicity (dashed lines, shifted by $+5000$ K). Electron density structures are shown in the inset. Panel (b) displays the resulting differences between the ATLAS9 and TLUSTY temperature structures (in percent). Panel (c) and (d) compare the TLUSTY with ATLAS9 and ATLAS9+DETAIL Eddington fluxes, respectively. The insets highlight the regions around the Lyman and the Balmer jumps. Colour coding according to the legends.

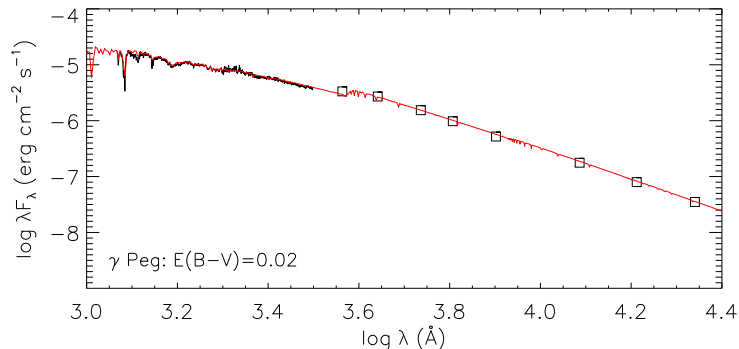


Figure 3. Comparison between our computed SED (red line) and observation for γ Peg (B2 IV): IUE spectrophotometry (black line) and UBVRIJHK photometry (squares).

the ATLAS9 than in the TLUSTY model, resulting in a stronger line-blanketing effect, exactly as indicated in Fig. 2 (a). Very good agreement is found also for LTE and NLTE density structures. Overall, close agreement of the LTE and NLTE structures is found over the entire parameter range considered, for the depths relevant for the formation of the observable line spectra and continua, at $-2 \lesssim \log m \lesssim -0.3$.

As temperature and density stratifications are not directly observable, we verified the effects on line profiles of hydrogen, helium and metal lines by performing line-formation computations with DETAIL & SURFACE on ATLAS9 and TLUSTY atmospheres. Indeed, only small differences are found for the resulting profiles, which are irrelevant for the stellar parameter and elemental abundance determination, see e.g. Fig. 10 of [24]. Maximum effects on metal abundances derived from a few individual lines are about 0.05 dex, and less for mean elemental abundances.

Overall good agreement is also found for the LTE and NLTE spectral energy distributions (SEDs), as exemplified in Fig. 2 (c) and (d). The differences in the continua are because of the temperature differences at the formation depths. Significant discrepancies occur only in the Lyman and helium continua, but it is difficult to test the models in this respect as interstellar absorption prevents observations of the extreme-UV for almost all early-type stars. The model differences in the extreme-UV vary with T_{eff} . Very good agreement over the entire spectral range is achieved at higher T_{eff} , see Fig. 9 of [24]. Our models can reproduce observed SEDs and therefore the global stellar energy output very well, if the observations are corrected for the appropriate amount of interstellar reddening. An example, for γ Peg, is shown in Fig. 3.

We conclude that *LTE and NLTE model atmospheres are essentially equivalent for dwarf and giant stars over the range $15\,000 \leq T_{\text{eff}} \leq 35\,000$ K*, for most practical applications.

Line spectra. Resolved line spectra are the most valuable observables as they give information about the temperature and density stratifications within the stars' atmospheres. They are also well-suited for the determination of stellar parameters and elemental abundances.

H & He: Hydrogen and helium provide the deepest features in the spectra of early B-type stars, thus sampling the widest extent of the atmospheric stratification. Our overall best-fit ADS model is compared to observed profiles for many diagnostic lines of γ Peg in Fig. 4. We note explicitly, that *one* synthetic spectrum is displayed in all the individual panels – also for all following comparisons – and not best fits to the individual lines. Overall, an excellent match of observation and theory is obtained. In particular the line wings agree well, being formed in the deeper layers of the atmosphere. Small discrepancies are present for the line cores, in particular for the stronger He I lines, which originate at shallower atmospheric depths. And, apparently the treatment of the He I forbidden components may be improved in some cases.

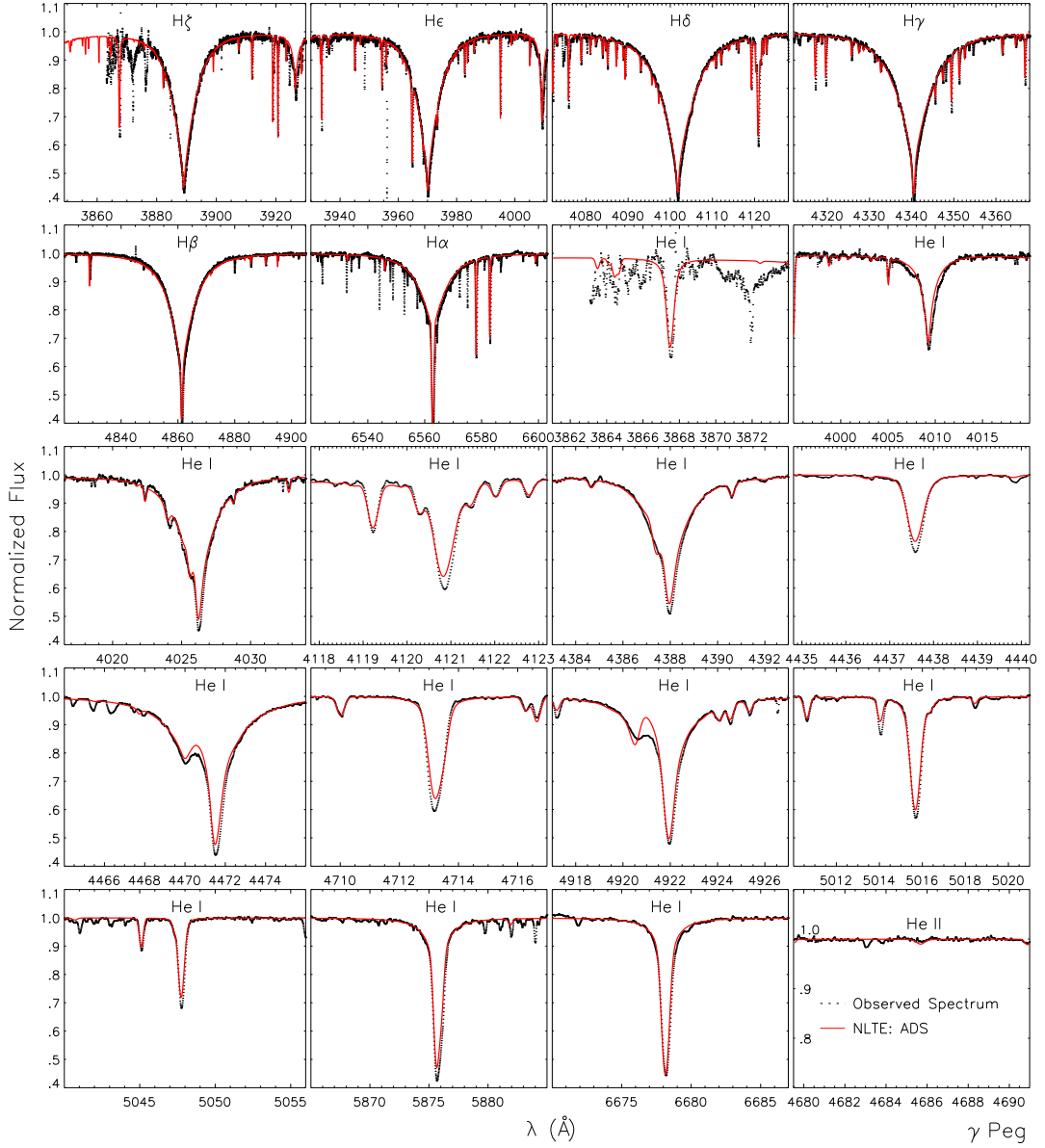


Figure 4. Comparison of strategic H I and He I/II in the observed spectrum of γ Peg (black dots) with our global best-fit ADS model (red line).

About the same fit quality can be achieved throughout the entire parameter space investigated here, with additional minor complications arising at the hotter end of the T_{eff} -range, where weak stellar winds start to impact H α and the He II $\lambda 4686 \text{ \AA}$ line, see [24] for examples.

We conclude that the NLTE modelling with ADS can reproduce the observed H I and He I/II lines reliably, except for some fine details. ADS models thus provide a good reference for the second step of our test, comparison with the TLUSTY/SYNSPEC NLTE and ATLAS9/SYNTHETIC LTE models, which is shown in Fig. 5. Both NLTE approaches produce closely resembling profiles for this test case, and the good agreement (except for some minor details) holds throughout the entire parameter range considered here for the H I, He II and He I triplet lines. However, at higher temperatures the He I singlet lines computed with TLUSTY/SYNSPEC become significantly weaker than the ADS profiles (and the observations) – the well-known singlet-triplet problem [30].

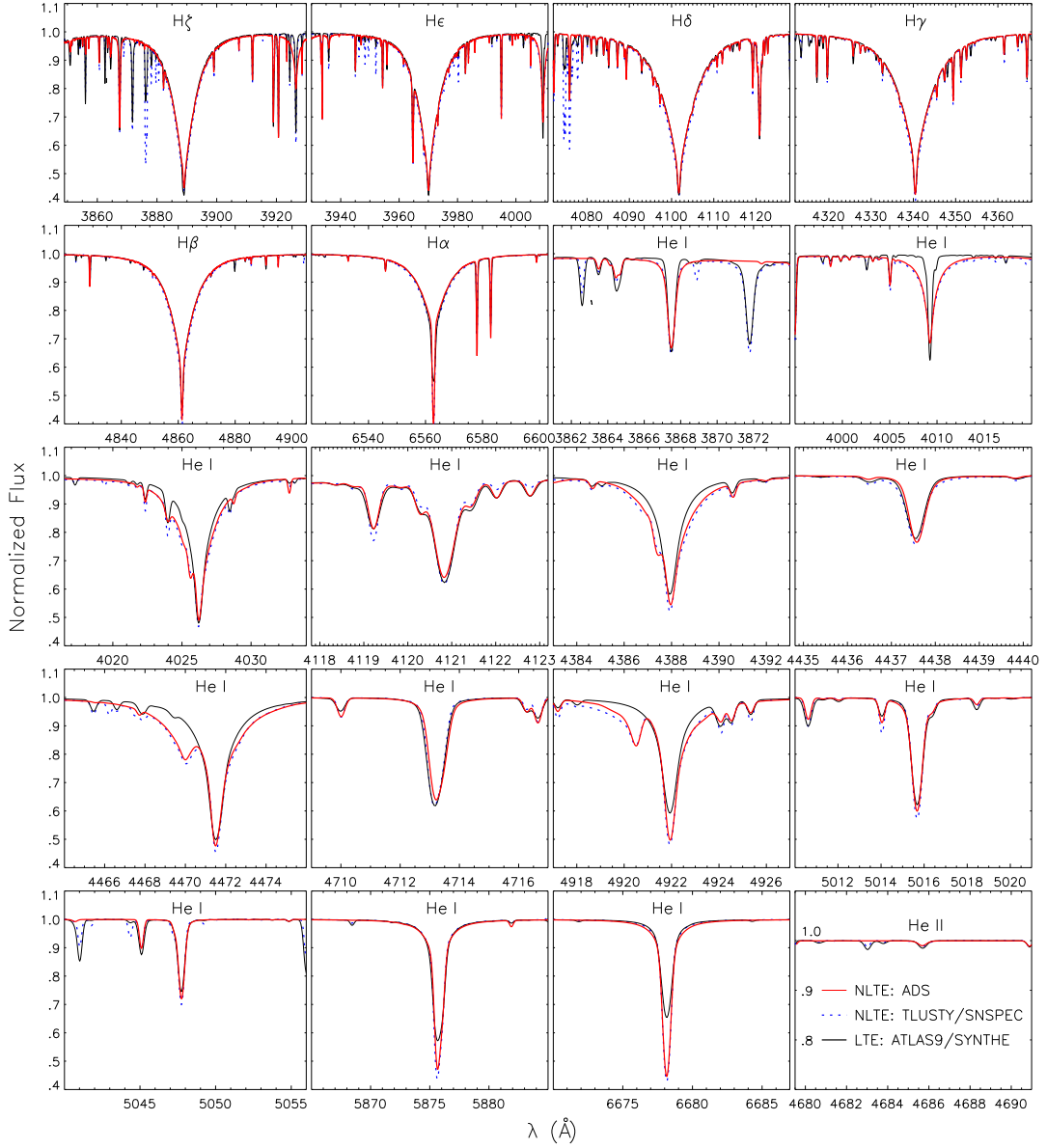


Figure 5. Same as Fig. 4, comparing line profiles computed with ADS, TLUSTY/SNSPEC and ATLAS9/SYNTH (line designations according to the legend).

Good agreement between the NLTE models and the ATLAS9/SYNTH profiles is found for the Balmer lines and a few sharp He I lines, *for this test case*. However, problems with inadequate line broadening – Voigt profiles with constant Stark broadening parameter and no account for forbidden components – are indicated for the majority of the He I features (in particular all diffuse ones) computed with ATLAS9/SYNTH. This can be resolved simply by implementing the appropriate broadening tables. More fundamental are the discrepancies in the depths of lines such as He I $\lambda\lambda$ 4921, 5875 and 6678 Å, which are genuine NLTE effects.

The comparison over the entire parameter range reveals severe shortcomings of LTE modelling of observed hydrogen and helium lines. Over the T_{eff} -range of 22 000 to 25 000 K, NLTE effects quickly set in and affect the cores and wings of the Balmer lines, and subsequently all helium lines. Maximum effects are found for highest T_{eff} : the Balmer lines computed in LTE have

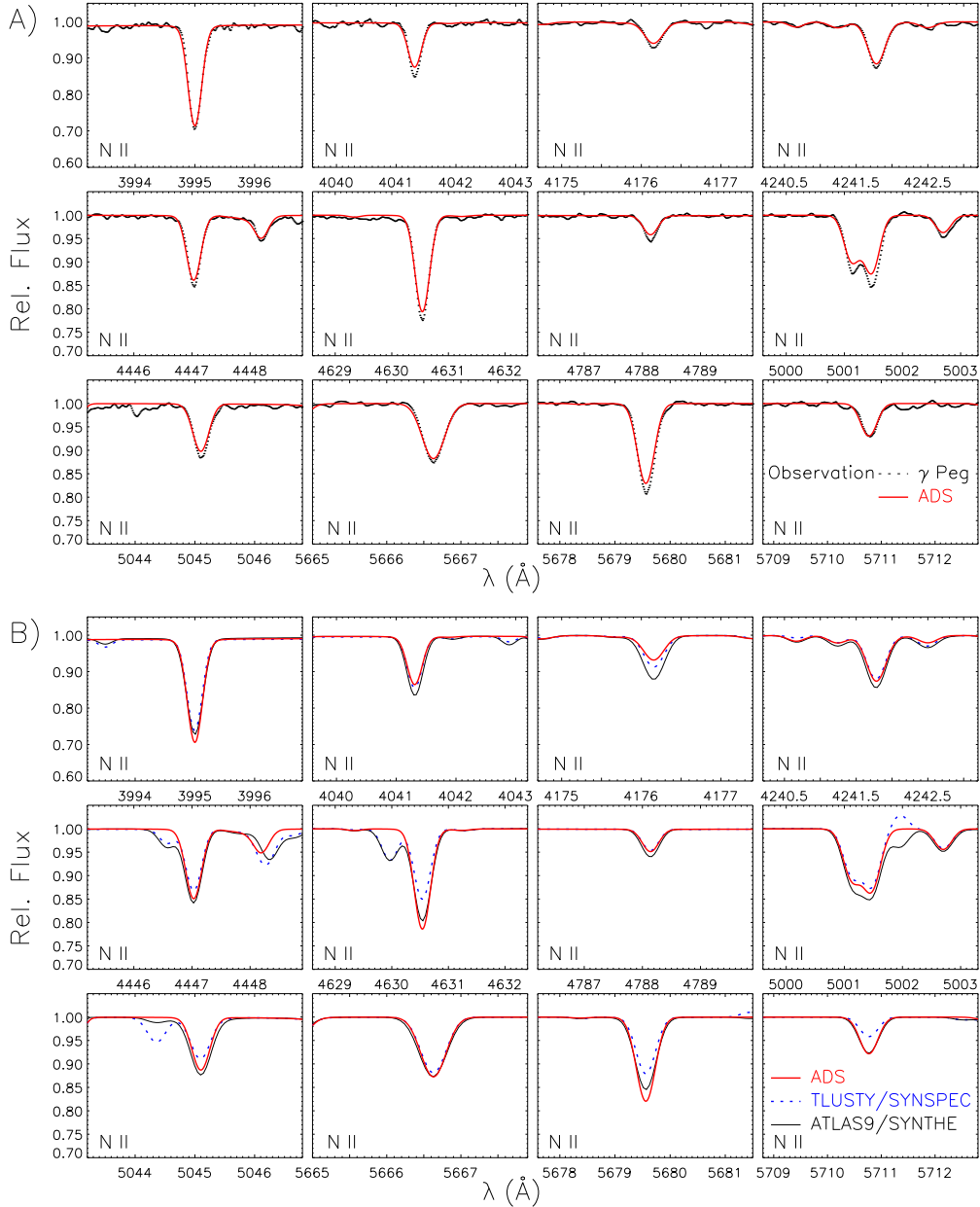


Figure 6. A): comparison of observations for N II lines in γ Peg with our global best-fit ADS model. B): comparison of ADS, TLUSTY/SYNSPEC and ATLAS9/SYNTH models for the same lines. See figure legends and the text for details.

equivalent widths about 30% lower than in NLTE, and up to a factor of more than 2 for the He I lines. Surface gravities determinations based on Balmer-wing fitting is thus subject to systematic error, e.g. $\log g$ values are overestimated by up to 0.2 dex from LTE analyses of H γ .

Overall, LTE modelling of the Balmer wings and selected He I lines appears to be largely unbiased by systematic error for main sequence stars up to $T_{\text{eff}} \simeq 22\,000$ K. Preference should then be given to the He I $\lambda\lambda 3867, 4121, 4437, 4713, 5016$ and 5048 \AA transitions, which are least affected by NLTE effects. Either full or hybrid NLTE models have to be used for quantitative analyses of stars at higher T_{eff} when systematic bias is to be avoided. Our ADS approach improves on the TLUSTY OSTAR2002/BSTAR2006 grids by avoiding the He I singlet-triplet problem.

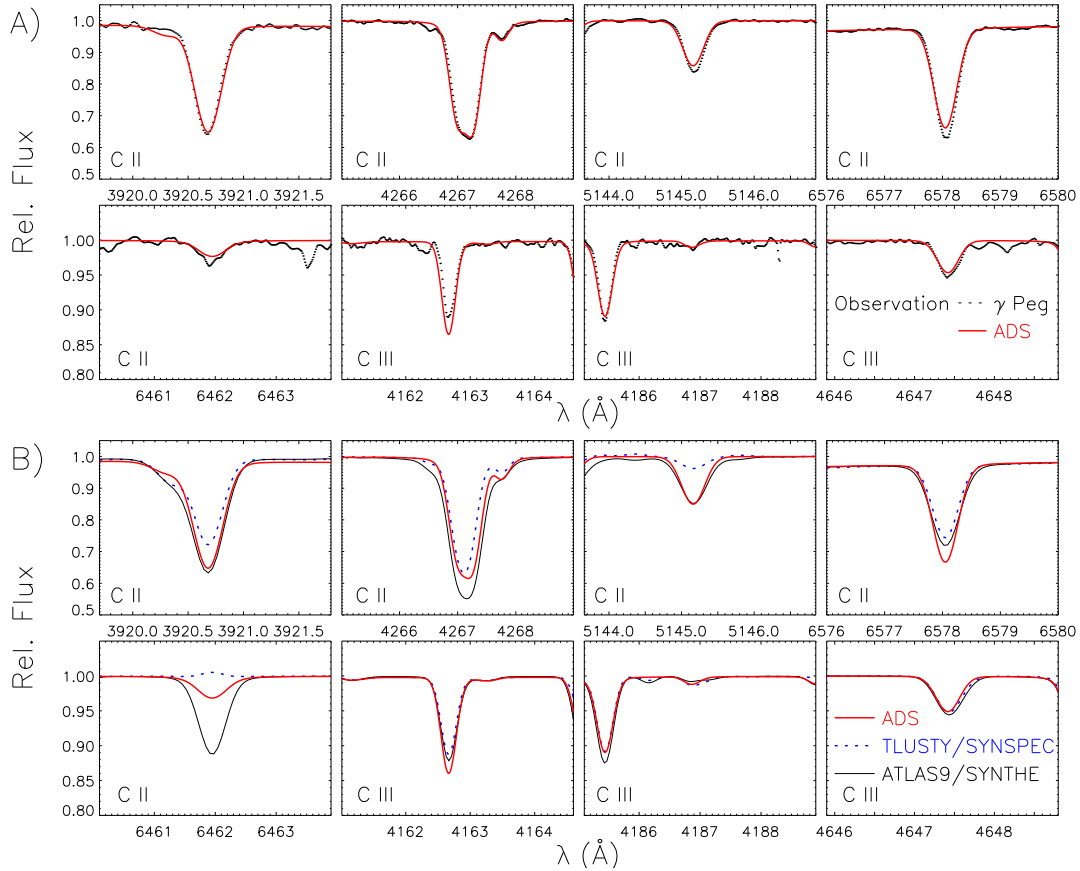


Figure 7. As Fig. 6, for C II/III lines.

Nitrogen: We discuss here only spectral lines of the N II ion, which in contrast to N III lines are observable throughout the entire parameter range. A comparison of important diagnostic lines in the optical spectrum of γ Peg with our global best-fit ADS model is shown in Fig. 6. The fit quality is excellent, in total 40 N II lines were analysed to derive the mean nitrogen abundance. Therefore, the ADS model provides a good reference for the comparison with the other codes, which is shown in the bottom half of Fig. 6.

In many cases good agreement is found between the TLUSTY/SYNSPEC and ADS NLTE line profiles. However, a significant number of differences exists, e.g. for N II $\lambda\lambda$ 4630, 5045, 5679 and 5711 Å from the examples shown in Fig. 6, where the TLUSTY/SYNSPEC models are too weak compared to observation. Abundance analyses based on such features would therefore significantly overestimate the nitrogen abundance. Both agreement and discrepancies vary throughout the entire parameter range considered here, so that it is difficult to quantify them in brief. In general, the differences increase towards lower gravities. The reasons for the differences in the two NLTE approaches result almost entirely from the model atom implementations. We tested this by adopting the N II model atom used in the TLUSTY computations for DETAIL/SURFACE and could tightly reproduce the TLUSTY/SYNSPEC solution.

The comparison of the NLTE ADS reference with the LTE ATLAS9/SYNTH model shows that NLTE effects are often small, except for lines such as N II λ 4176 Å from the examples. In fact, ATLAS9/SYNTH profiles are closer to the ADS profiles (and therefore observation) than the TLUSTY/SYNSPEC profiles in most cases. The NLTE effects become more pronounced with decreasing surface gravities.

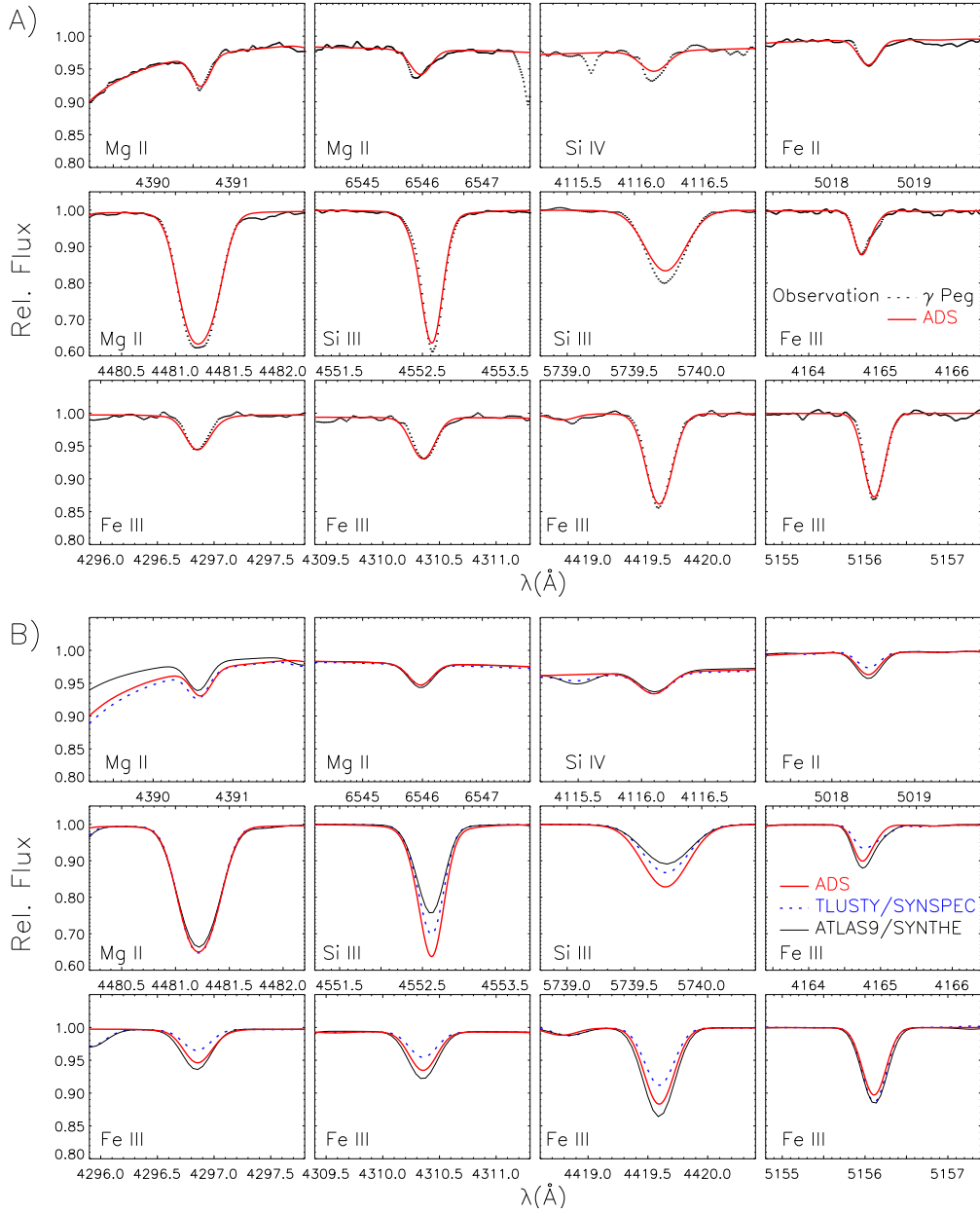


Figure 8. As Fig. 6, for Mg II, Si III/IV and Fe II/III lines.

Oxygen: We investigated the behaviour of O I and O II lines, with similar results to those for nitrogen. Because of this we omit a more detailed description here. Noteworthy are the overall relatively small NLTE effects, again with the exception of several multiplets, e.g. the near-IR triplet O I $\lambda\lambda 7771-5$ Å. For these lines, large differences between the two NLTE solutions are seen, again probably because of the different model atom implementations.

Carbon: Singly and doubly-ionized carbon were investigated. Again, the ADS model provides a good reference for further comparison with other models, as it reproduces observation well, not only for γ Peg (see examples in Fig. 7) but throughout the entire early B-type main sequence [16].

In particular C II was known as one of the most challenging cases for NLTE line formation computations for decades. The comparison of ADS with the TLUSTY/SYNSPEC solution shows

disagreement in practically every line. Usually the TLUSTY/SYNSPEC profiles are too shallow, and in some cases even turn into (unobserved) emission (C II $\lambda 6462$ Å). The situation is much better for C III, except for the strong line C III $\lambda 4162$ Å. The problems with C II persist for other parameter combinations. Certainly, the TLUSTY model atom for carbon needs to be improved to allow for meaningful abundance determinations. For the moment, C III should be preferred for abundance work based on the BSTAR2006 and OSTAR2002 grids.

The comparison with the LTE profiles shows that most of the stronger, but also several of the weak lines show pronounced NLTE effects, throughout the entire parameter range. An exception is C II $\lambda 5145$ Å (and its other multiplet members), which stays in LTE for all cases of interest. NLTE effects on the C III lines increase significantly for higher T_{eff} .

Magnesium, silicon and iron: Examples for the comparison of our global best-fit ADS model with observations for important diagnostic Mg II, Si III/IV and Fe II/III lines in γ Peg are shown in Fig. 8. The Mg II and Fe II/III are reproduced reliably. We are at present incorporating a new silicon model atom, in particular to improve the fits to several lines not shown here, but the old model [21] reproduces lines such as those of the Si III $\lambda\lambda 4552$ – 4575 Å triplet or Si IV $\lambda 4116$ Å reasonably well, providing a valuable diagnostic for T_{eff} -determination via the ionization balance.

Both NLTE solutions, with ADS and with TLUSTY/SYNSPEC, agree well for Mg II, but disagree for almost all Si and Fe lines. This is of concern in the case of silicon as use of the ionization equilibrium would lead to systematically different solutions for T_{eff} and $\log g$ with the BSTAR2006 and OSTAR2002 grids, probably inconsistent with other diagnostics. Moreover, the Si III triplet is often used to constrain the microturbulence velocity, which therefore may also become subject to systematic offsets when based on the TLUSTY grids. The iron lines are systematically shallower in the TLUSTY/SYNSPEC models, implying the derivation of higher iron abundances in applications. Because of the rôle of iron as the main line-opacity source this has further effects on atmospheric structure computations and therefore also on the atmospheric parameter determination. It is highly important to improve these model atoms for TLUSTY.

While the LTE and NLTE solutions for Mg II are very similar for the parameters of γ Peg (Mg II $\lambda 4390$ Å apparently differs because of its location in the wing of an ill-fitted He I line), the iron lines are weakly and most of the silicon lines strongly NLTE affected. LTE modelling of silicon lines in early B-type stars can lead to systematic errors in atmospheric parameters when using ionization equilibria, and to unreliable elemental abundances. LTE iron abundances are in general somewhat underestimated.

5. Conclusions and Recommendations

We have seen that the data from the Gaia mission will need to be complemented by ground-based (optical) spectroscopy for early-type stars in order to put meaningful constraints on atmospheric parameters and elemental abundances. Three approaches for the modelling of stellar atmospheres in the T_{eff} -range of 15 000 to 35 000 K, corresponding to spectral types of about B4 to O9, have been tested here: full LTE (with ATLAS9/SYNTH3), full NLTE (TLUSTY/SYNSPEC) and hybrid NLTE (ADS). The aim of the work was to determine the best means, presently available, to analyse optical spectra of such early-type stars, which is of course of much broader relevance than for Gaia-related science alone.

The comparison showed that pure LTE modelling can yield meaningful results for the low- T_{eff} regime, up to about 22 000 K on the main sequence, *if the right spectroscopic indicators are employed*. An overall good global match between synthetic and observed spectra cannot be expected to be obtained as many lines show NLTE effects.

Pure NLTE modelling with the available TLUSTY/SYNSPEC grids is conceptually superior. However, NLTE atmospheric structures and SEDs turn out to be close to LTE in the parameter space considered. NLTE line spectra of ions with ‘simple’ atomic structures, like H I, He I/II (with some restrictions at higher T_{eff}) or Mg II turn out to be reliable. However, oversimplified model

atoms cause problems for many of the more complex ions/elements. Blind use of the synthetic spectra published in the OSTAR2002 and BSTAR2006 grids should therefore be avoided. *The fact is that NLTE computations based on inappropriate model atoms can potentially introduce larger systematic errors to quantitative analyses than simple LTE modelling.* The TLUSTY model atoms certainly need extensive revision before a good global match with observations can be obtained with this package.

Our NLTE line-formation computations with DETAIL/SURFACE on ATLAS9 atmospheres combine the advantage of low to moderate CPU time requirements with realistic model atoms, facilitating a robust global match of observed spectra to be obtained, see also [27, 28]. It is reassuring that the same model atoms provide as good a match of the synthetic spectra to observations also for other kinds of stars, with drastically different chemical composition such as subdwarf OB stars [31] or extreme helium stars [32, 33, 34]. First applications of our models combined with a sophisticated analysis methodology promise breakthroughs for several astrophysical fields, see e.g. [25].

References

- [1] Kurucz R L 1993 *CD-ROM No. 13* (Cambridge, Mass.: SAO)
- [2] Kurucz R L and Avrett E H 1981 *Solar Spectrum Synthesis. I. A Sample Atlas from 224 to 300 nm*, SAO Spec. Rep. **391** (Cambridge, Mass.: SAO)
- [3] Hubeny I and Lanz T 1995 *ApJ* **439** 875
- [4] Giddings J R 1981 *Ph.D. Thesis* (Univ. London)
- [5] Butler K and Giddings J R 1985 *Newsletter of Analysis of Astronomical Spectra*, No. 9 (Univ. London)
- [6] Blomme R 2011 *J. Phys.: Conf. Series* (these proceedings)
- [7] Groh J H 2011 *J. Phys.: Conf. Series* (these proceedings)
- [8] Castelli F and Kurucz R L 2003 *Proc. 210th IAU Symposium* ed N Piskunov et al. (San Francisco: ASP) p A20
- [9] Munari U, Sordo R, Castelli F and Zwitter T 2005 *A&A* **442** 1127
- [10] Lanz T and Hubeny I 2003 *ApJS* **146** 417
- [11] Lanz T and Hubeny I 2007 *ApJS* **169** 83
- [12] Rybicki G B and Hummer D G 1991 *A&A* **245** 171
- [13] Przybilla N and Butler K 2004 *ApJ* **609** 1181
- [14] Przybilla N 2005 *A&A* **443** 293
- [15] Nieva M F and Przybilla N 2006 *ApJ* **639** L39
- [16] Nieva M F and Przybilla N 2008 *A&A* **481** 199
- [17] Przybilla N and Butler K 2001 *A&A* **379** 955
- [18] Przybilla N, Butler K, Becker S R, Kudritzki R P and Venn K A 2001 *A&A* **359** 1085
- [19] Becker S R and Butler K 1988 *A&A* **201** 232
- [20] Przybilla N, Butler K, Becker S R and Kudritzki R P 2001 *A&A* **369** 1009
- [21] Becker S R and Butler K 1990 *A&A* **235** 326
- [22] Becker S R 1998 *ASP Conf. Ser.* **131** 137
- [23] Morel T, Butler K, Aerts C, Neiner C and Briquet M. 2006 *A&A* **457** 651
- [24] Nieva M F and Przybilla N 2007 *A&A* **467** 295
- [25] Nieva M F, Przybilla N and Irrgang A 2011 *J. Phys.: Conf. Series* (these proceedings)
- [26] Przybilla N, Nieva M F and Butler K 2008 *ApJ* **688** L103
- [27] Nieva M F and Simón-Díaz S 2011 *A&A* **532** A2
- [28] Nieva M F and Przybilla N 2011 *A&A* (submitted)
- [29] Grevesse N and Sauval A J 1998 *Space Sci. Rev.* **85** 161
- [30] Najarro F, Hillier D J, Puls J, Lanz T and Martins F 2006 *A&A* **456** 659
- [31] Przybilla N, Nieva M F and Edelmann, H. 2006 *Balt. Astron.* **15** 107
- [32] Przybilla N, Butler K, Heber U. and Jeffery C. S. 2005, *A&A* **443** L25
- [33] Przybilla N, Nieva M F, Heber U. and Jeffery C. S. 2006, *Balt. Astron.* **15** 163
- [34] Kupfer T, Heber U, Przybilla N, Jeffery C S, Behara N T and Butler K 2010 *AIP Conf. Proc.* **1273** 209